2015

The Effect of 3D Collagen Scaffolds on Regulating Cellular Responses

Chad Simmons
University of South Carolina

The Effect of 3D Collagen Scaffolds on Regulating Cellular Responses

by

Chad Simmons

Bachelor of Science
University of South Carolina, 2012

Submitted in Partial Fulfillment of the Requirements

For the Degree of Master of Science in

Biomedical Science

School of Medicine

University of South Carolina

2015

Accepted by:

Jay Potts, Director of Thesis

Wayne Carver, Reader

Richard Goodwin, Reader

Lacy Ford, Senior Vice Provost and Dean of Graduate Studies

Dedication

To my parents: Ada and Herbert Simmons. Thank you for all of the love and support you have given me.

Acknowledgements

I would like to thank Dr. Jay Potts, for being my mentor and guiding me in the creation of this thesis. I want to thank the members of my thesis committee: Dr. Richard Goodwin and Dr. Wayne Carver for their assistance in revising my thesis and taking part in my thesis defense. I want to thank the staff of the IRF: Dr. Robert Price, Anna McNeal, Lorain Junor, and Jeff Davis for teaching me how to use the equipment in the IRF. Lastly, I want to thank the current and previous members of Dr. Potts' lab: Dr. Keith Moore, Adam Vandergriff, Brian Bennett, Edgar Macal, Marwa Belhaj, and Vinal Menon, for helping me in the defense of my thesis and instructing me on lab techniques when I joined Dr. Potts' lab.

Abstract

Epithelial cells, as well as other differentiated cell types, remodel surrounding collagen in vitro, to self organize into 3D structures. When placed on-top or inside of a collagen hydrogel, cells organize into a toroid or spheroid form. It is not clearly understood how these cell types modulate surrounding collagen to form 3D shapes. The goal of this project was to determine if cell type, collagen type, or cell placement are factors that can alter how cells reorganize and remodel collagen hydrogels. We hypothesize that the positioning, cell type and the type of collagen they are in contact with affect the 3D reorganization of cells in collagen. Staining the cell nuclei, the actin cytoskeleton and monitoring cell proliferation provided better insight as to how cells organize over time in collagen hydrogels. Alpha smooth muscle actin and vimentin proteins were targeted to identify the shapes of cells in the hydrogels. Hydrogel thickness measurements and cell alignment studies were done to monitor the modulation of collagen over time and determine if patterns of cellular organization were present throughout the hydrogel. When placed on-top of a collagen hydrogel, rat neonatal heart fibroblasts (rat NHFC) modulated type I and type III collagen hydrogels into toroidal forms. Rat tail collagen hydrogels shrank when rat NHFCs were interspersed inside. However, unlike other inside placed cellular hydrogels, rat NHFC placed inside of a human type III collagen hydrogels developed ring shaped cellular alignments around the edges of the hydrogel. Rat NHFCs can modulate human type III collagen in a different manner than that with rat tail

collagen. Unlike the rat NHFC, the mouse breast cancer cell line 4TI-LUC did not form toroids or remodel collagen when placed on top or inside of a collagen hydrogel. Cancer inhibits the migration and reorganization processes observed in non-cancerous cell types. Hence, there seems to be a universal process involved when non-cancerous cells interact with a collagen hydrogel when placed on the surface.

Table of Contents

List of Figures

Chapter 1: Introduction

Self-assembling tissue structures are cells and that can aggregate to form a specific shape or form. Such structures can congregate and manipulate a collagen environment to adopt various three dimensional (3D) forms. Rabbit lens epithelial cells (RLEC) and rat neonatal heart fibroblast cells (rat NHFC) are differentiated cell types that have the ability to from hollow, densely packed, ring shaped 3D structures called toroids when placed on top of a collagen hydrogel (Gourdie 2011). After toroid formation, the hydrogels curve inward to form a spherical shape called a spheroid. When RLECs are placed inside a collagen hydrogel, the entire hydrogel contracts into a smaller circular shape regardless of its original shape (Gourdie 2011). Collagen hydrogels without cells do not contract or change shape in culture media over time. RLECs and other differentiated cell types form toroid shapes within twelve hours of interaction with the surface of a collagen hydrogel (Gourdie 2011). In both, inside and on-top collagen hydrogel environments, the amount of hydrogel contraction increases the longer the cells interact with the hydrogel (Gourdie 2011). Understanding how these cell types reorganize in collagen environments and having the ability to control that reorganization could lead to improvements in tissue engineering.

Collagen is a component of the mammalian body that is responsible for the biological and structural integrity of the extracellular matrix (ECM) (Cen 2008). Collagen has a triple helix structure that is made up of fibrils that consist of multiple monomers.

Collagen is derived from procollagen which is made up of globular C and N propeptides that are joined by their respective ends on a triple helix (DiLullo 2002). Type I procollagen is made up of 2 α_1 chains and 1 α_2 chain when secreted outside of a fibroblast. Outside of the cell, the propeptides are cleaved by C and N proteinases and the collagen monomer is assembled into a collagen fibril (DiLullo 2002). There are 28 known types of collagen, but the most common is type I collagen, which is the most abundant protein in humans and is responsible for supporting load bearing tissues like bones and tendons (DiLullo 2002). Type I collagen is a component of the ECM and is present in many intercellular interactions. There are collagen sequences that interact with type I collagen that facilitate cell adhesion, support binding to other matrix components, and regulate interactions with tissue calcification factors (DiLullo 2002).

Type III collagen is abundant in the skin arteries, and the intestine (Mizuno 2013). Type III collagen is a critical component of blood vessels, and provides support to the skin and bones. Deficiencies in the gene coding for type III collagen can lead to Ehlers-Danlos syndrome like characteristics in mice (Liu 1997). Type III collagen is very biocompatible, similar to type I collagen. Rats that had collagen hydrogels implanted into them for over six months had no adverse affects and the hydrogels were well tolerated and not toxic (Jeyanthi 1990). Sheets of non-crosslinked porcine collagen implanted into Wistar-Han rats did not impede cellular proliferation after 12 months of contact with the host tissue (de Castro Bras 2010). Hence, collagen constructs seem to be an ideal scaffold for implanting cells into the human body due to the biocompatibility and availability of collagen. Understanding how cells self assemble could benefit the development of tissue

and organ creation from isolated cells. Collagen is a very biocompatible substance that can be used to support artificial tissues and organs into the human body.

Determining how collagen is manipulated by self assembling tissue structures would be beneficial to the development of tissue engineered constructs. Collagen hydrogels are a very common scaffold for live cells due to the hydrogel emulating in vivo conditions and having various applications in tissue engineering (Antione 2014). Collagen hydrogels have been used in recent works to determine scaffold changes in response to cell proliferation and motility. Macromolecular crowding is a physiological state where macromolecules occupy space and contribute to a fractional volume occupancy (Dewavrin 2014). In vivo collagen can self assemble in solutions that are crowded with non-interacting macromolecules. Macromolecular crowding can be used to alter collagen fiber thickness and enhance stem cell proliferation in collagen hydrogels (Dewavrin 2014). By creating collagen and elastin hybrid hydrogels, lung fibroblasts interact and combine to match the theoretical value (the density of a normal human lung ≈5 kDa) of an avleolar wall (Dunphy 2014). Human neural precursor cells have improved neurite outgrowth when inside a 3D collagen hydrogel microenvironment with umbilical cord blood cells (Park 2014). The toroids formed from cells placed on top of collagen hydrogels could be used to create cylindrical vessels (Gourdie 2011). Collagen is a biocompatible substance that has a lot of utilities ranging from implantation to improving cellular proliferation. Determining how cells react in a collagen environment can improve the development of three dimensional tissue structures by controlling intercellular shifts and interactions.

The phenomenon of cellularized hydrogels forming distinct shapes can be considered a process of self assembly. Self-assembly is the autonomous organization of components into patterns or structures without intervention (Whitesides 2002). There are two main forms of self-assembly: static and dynamic (Whitesides 2002). The majority of research done with self assembling tissue structures are of the static variety. Static self-assembling tissue structures involve systems that are at a global or local equilibrium and do not dissipate energy (Whitesides 2002). An object is at equilibrium when the net force applied to the object is 0. The only forces that are applied to the collagen hydrogels in this project are from the cells placed inside or on-top of them. The hydrogels remain in equilibrium because the forces applied to the hydrogels by the cells do not cause the hydrogel to move. The overall shape of the hydrogel changes, but no directional movement occurs. The dissipation of energy is a physical process where energy becomes unavailable and irrecoverable in any form, similar to how the kinetic energy applied to a pool ball is lost from being in constant contact with the surface of the pool table. Self-assembling tissue structures are present in both histogenesis and organogenesis (Jakab 2004). Cells and tissues that self assemble are utilized in fetal development and wound healing to develop functional tissues and maintain homeostasis. Multicellular systems such as cellular aggregates or "bio-ink" are also considered self-assembling tissue structures. Cell-to-cell and cell-to-ECM interactions are critical in the development of a tissue structure. Understanding how self-assembling tissue structures function and interact is a vital component needed to create biocompatible tissues. The knowledge gained from utilizing self-assembling tissue structures can be used to obtain a greater

understanding of mammalian development, and can lead to further developments in preventative medicine.

The ECM plays a vital role in cell migration and communication. The ECM is mainly composed of water, proteins, and polysaccharides. The ECM is a highly dynamic environment that undergoes constant remodeling (Frantz 2010). Integrins and discoidin domain receptors are mediators that can regulate cell adhesion to the ECM (Frantz 2010). Fibrous proteins and proteoglycans are the two main classes of macromolecules that form the ECM (Frantz 2010). Collagen is one of the fibrous proteins that is present within the ECM. Collagen levels vary depending on the cell type and the environment of the cell. Collagen is the most abundant fibrous protein found within the interstitial ECM and constitutes up to 30% of the total protein mass of multicellular animals (Frantz 2010). ECM interconnections enable cellular movement and intercellular signaling. The basal lamina, a specialized form of extracellular matrix that are under epithelial cell sheets are involved in maintaining structure of tissue: can direct cell migration and support cell proliferation. Fluctuations in the shape of the ECM allow for multiple interactions between multiple cells. Structures like the basal lamina can alter and direct how cells proliferate and align, making it an important part of wound healing.

Epithelial to mesenchymal transition (EMT) is a process where fully differentiated epithelial cells transition to a mesenchymal phenotype (Dong 2014). More specifically, EMT is a biological process where a polarized epithelial cell undergoes multiple biochemical changes that enable it to assume characteristics of a mesenchymal phenotype, such as migration, invasiveness, increased ECM production, and an increased resistance to apoptosis (Kalluri 2009). The mesenchyme is made up of a collection of

loose cells and proteins that are involved in the development of morphological structures in developing embryos. Vimentin and fibroblast-specific protein 1 (FSP-1), markers of mesenchymal cells, are found in migrating epithelial cells on the edges of a wound around 10 to 15 days after injury (Yan 2010). The appearance of mesenchymal cells at the edges of wounds, but not in other areas of the skin, is a characteristic that is only seen during wound healing. Intercellular interactions regulate the occurrence of EMT in the repair of epithelial damage. The transition from epithelial to mesenchymal cells types may provide insight as to how differentiated cell types migrate and reorganize in to 3D forms.

Imaging self assembling tissue structures interspersed at different regions of a collagen hydrogel will provide a glimpse as to how positioning influences cell movement during contraction. Alpha smooth muscle actin (α-SMA), the cell proliferation marker Ki-67, and vimentin, a marker for EMT were observed in RLEC and rat NHFC collagen hydrogels. α SMA, a marker for EMT (Kalluri 2009), is present in vascular smooth muscle cells and is a main factor in cell movement and morphology. Vimentin is a protein found in the intermediate filaments that make up the cytokeleton of normal mesenchymal cells (Satelli 2011). Vimentin knockout mice have pups that have fibroblasts that are weak and experience reduced migration and 3D collagen contraction (Eckes 2000). Ki-67 is marker for cellular proliferation found on the surface of chromosomes located in the nuclei of cells during mitosis and in the nucleus during interphase (Schlozen 2000). The Ki67 antigen is found in cells that are in the G_1,S,and G_2 stages of the cell cycle, but are absent from cells in the G_0 stage (Scholzen 2000). These three markers are critical in understanding how differentiated cell type such as RLECs

and rat NHFCs manipulate collagen environments. Determining which cells display proliferation, movement, and observing their overall shape can lead to understanding the interactions that take place between RLEC and rat NHFC during toroid and spheroid formation in collagen hydrogels. By taking confocal images of the different hydrogel types, measuring the thickness of specific points of each hydrogel, and monitoring the alignments of the cells inside the hydrogel, this study reveals the mechanisms that differentiated cell types use to manipulate collagen.

Collagen is a useful scaffold both for testing how cells interact with each other in vitro, as well as a material to introduce cells into a living organism. By researching and finding methods that can manipulate how self assembling tissue structures modify a collagen environment, improvements can be made to existing tissue and organ engineering projects. Studying EMT, cell shape, and cell proliferation in hydrogels with RLEC or rat NHFC can show how these cell types modify collagen to form ECM interconnections and utilize collagen in vitro. Our lab suggests that the type of collagen and the positioning of the cells with respect to collagen affect how differentiated cell types reorganize in collagen. The main purpose of this study was to analyze how different cell types modified type I and type III collagen hydrogels and determine if there are any patterns or occurrences that promote or control toroid and spheroid formation.

Chapter 2: Methods

Chapter 2.1: Cell Culture of Self Assembling Tissue Structures

Rat NHFC are the main cell type used in this project. The rat NHFC were isolated from grinding the hearts of 3 to 5 day old rats. The pieces of heart are digested with collagenase and the cells remaining are placed into culture dishes for an hour. The cells that attached to the plastic culture dish were fibroblasts. Fibroblasts were separated from the remaining heart components placed in another culture dish with media until only the fibroblasts remain. The rat NHFCs were cultured in T-200 culture flasks using normal (4.5g/L of glucose) DMEM at a pH of 7.4 supplemented with 10% FBS, gentamyacin, streptomycin, and amphoteracin B. The cells were cultured at a temperature of 37°C and 5% CO_2. Once the cells were confluent, the media was aspirated from the flask and the cells were rinsed in Mosconas solution (pH of 7.5). The Mosconas solution was aspirated from the flask and 3 ml of 0.25% Trypsin/EDTA (pH of 8.1) was added to the cells (10 ml of 0.25% Trypsin/EDTA for Rat NHFC). Culture flasks were incubated at room temperature for 2 minutes and shaken gently at regular intervals until all of the cells were detached from the flasks. The cell and trypsin mixture was removed from each flask and placed in a 50ml conical tube. Culture media was added to the tube and the cells were spun down to form a pellet in a centrifuge set to 700 RCF for 8 minutes. After centrifugation, the media and trypsin mixture was aspirated from the tube without

disturbing the pellet of cells at the bottom. Culture media was used to re-suspend the cells. The suspended cells were either split into two different culture flasks for further culturing or were used immediately in conjunction with polymerized collagen hydrogels for contraction assessments. Rat NHFC that were used for cellularized hydrogels were between passage 9 and 17.

Chapter 2.2: Collagen Hydrogel Construction

Two variations of hydrogels were used in this study: a collagen hydrogel that contained cells mixed inside and a polymerized collagen hydrogel with cells placed on-top of its surface. This study utilized two different hydrogel compositions: rat tail collagen and human type III collagen.

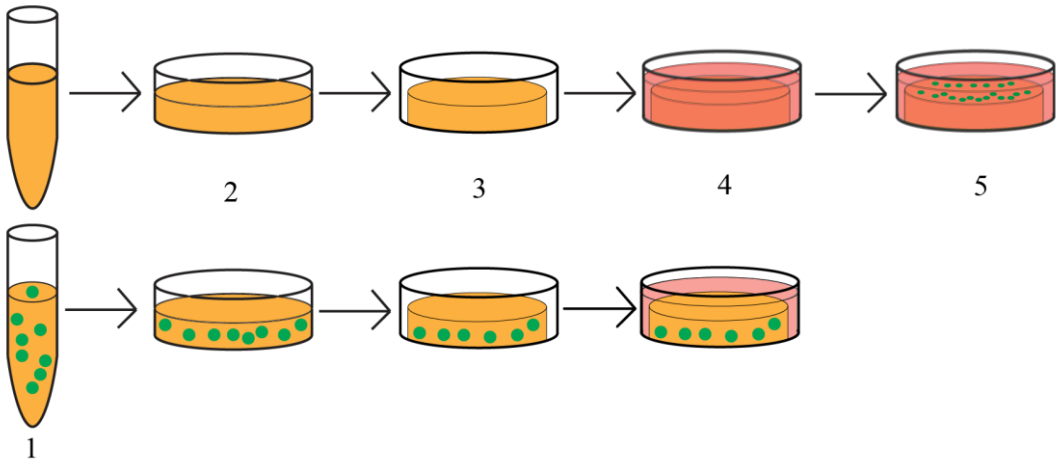

Figure 2.1: This image represents the creation of on-top hydrogels (top row) and inside hydrogels(bottom row).

Table 2.1: Step by Step Specifics on Collagen Hydrogel Creation

On-Top Hydrogel Creation	**Inside Hydrogel Creation**
1. Depending on the type of collagen used a mixture of the collagen hydrogel components were made (in Table 2.2).	1. Depending on the type of collagen used a mixture of the collagen hydrogel components were made (in Table 2.2) and the exact amount of cells were added

	to the collagen hydrogel mixture and thoroughly mixed together (1 x 10^6 cells per ml of hydrogel mix).
2. A specific amount of the mixture was placed into multiple wells of a 24 well plate and polymerized at 37°C for 1 hour.	2. A specific amount of the mixture was placed into multiple wells of a 24 well plate. The mixture polymerized at 37°C for 1 hour.
3. After the hydrogels polymerized, a p20 pipette tip was used to scrape around the circumference of each hydrogel to separate it from the walls of the plate.	3. After the hydrogels polymerized, a p20 pipette tip was used to scrape around the circumference of each hydrogel to separate it from the walls of the plate.
4.Culture media specific to that cell type was added to the hydrogel, until the entire hydrogel was submerged in media.	4.Culture media specific to that cell type was added to the hydrogel, until the entire hydrogel was submerged in media.
5. The cells suspended in media were added to the top of the collagen hydrogel in slow droplets (1 x 10^6 cells per ml).	5.The hydrogels were placed back inside the incubator until a specific time point was reached.
6. The hydrogels were placed back inside the incubator until a specific time point was reached.	

Dialyzed rat tail collagen and human type III collagen had cells placed inside and on top of them. All Rat NHFC hydrogels were composed of 500 µl of hydrogel mix and each gel had 500,000 cells placed inside or on-top.

Table 2.2 Hydrogel compositions and cell types incorporated

Type of hydrogel	**Materials used**	**Ratio of materials used**	**Hydrogel sizes**
Rat NHFC Rat tail collagen hydrogel	Dialyzed rat tail collagen: sterilized water: filtered sodium bicarbonate (in deionized water): M199 Media	25:15:4:4	500 µl per well
Rat NHFC Type III collagen hydrogel	Advanced Biomatrix human collagen type III : 10X MEM : 0.2N HEPES	8:1:1	500 µl per well

Each hydrogel created was incubated at 37°C and 5% CO_2. Rat NHFC type III collagen hydrogels were made using purified human type III collagen (pH of 2), HEPES (pH of 9), and MEM (pH of 7.3). Rat NHFC human type III collagen hydrogels and rat NHFC rat tail collagen hydrogels were analyzed by confocal microscopy at 3, 6, 9, 12, 24, and 36 hour timepoints. Thickness measurements of inside and on-top rat tail collagen hydrogels were done in 6, 12, 18, and 24 hour timepoints.

Chapter 2.3: Hydrogel Fixation and Immunohistochemistry

At the desired time point, a digital camera was used to take an image of the hydrogel in PBS. First the media was removed and 500 µl of PBS was added to each hydrogel. After images of the hydrogels were taken, the PBS was removed and 1 ml of 2% paraformaldehyde in PBS (PFA/PBS) was added to each hydrogel and was removed after one hour of fixation. Once fixed, the hydrogels were washed three times for 10 minutes each in PBS. After the last wash, 1 ml of PBS was added to each well and the hydrogels were stored at 4°C until used for thickness measurements or confocal imaging. Before staining, whole fixed hydrogels were quartered with a razor blade to allow easier imaging of the center, middle and edge regions. Each hydrogel quarter was placed in a 24 well plate and all staining was done simultaneously.

Antibody staining was performed as previously published (Artym 2010). The cells on each quarter hydrogel slice were stained with DAPI to locate cell nuclei and an Alexa Fluor 488 Phalloidin stain was used to locate f-actin. The rat tail collagen rat NHFC hydrogels were stained with a monoclonal Cy3 conjugated anti vimentin antibody. The 3 to 36 hour type III collagen rat NHFC hydrogels were stained first with a polyclonal rabbit incubated Ki-67 primary antibody and then a goat-anti-rabbit Cy3

conjugated secondary antibody. All of the antibody dilutions were stored in 4°C prior to use. All staining took place at room temperature.

Table 2.3: Staining Protocol used for each hydrogel type

Rat NHFC rat tail collagen hydrogels	**Rat NHFC Type III collagen hydrogels**
1. Each hydrogel was washed with 0.5% Triton-X in PBS for 10 minutes.	
2. Each hydrogel was washed quickly with PBS.	
3. Each hydrogel was washed for 30 minutes in PBS.	
4. The hydrogels were blocked using 5% dry milk in de-ionized water for 30 minutes.	
5. Each hydrogel was washed for 10 minutes with PBS/Tween.	
6. 400 µl of DAPI[1:5000 in PBS] was added to each hydrogel. Hydrogels were stained for 1 hour	
7. Each hydrogel was washed 3 times for 10 minutes each in PBS/Tween	
8. 400 µl of 488 phalloidin [1:40 in PBS] was added to each hydrogel. Hydrogels were stained for 1 hour.	
9. Each hydrogel was washed 3 times for 10 minutes each in PBS/Tween	
10A. 300 µl of Cy3 conjugate anti vimentin antibody in PBS [1:100] was added to each hydrogel . Those hydrogels were stained for 1 hour.	10A. 400 µl of a polyclonal rabbit KI67 antibody in PBS [1:100] was added to each hydrogel. Each hydrogel was stained for 1 hour.
10B. Each hydrogel was washed 3 times for 10 minutes each in PBS/Tween	
	10C. 400 µl of a Cy3 conjugated goat anti-rabbit secondary antibody in PBS [1:100] was added to each hydrogel and stained for 1 hour.
	10D. Each hydrogel was washed 3 times for 10 minutes each in PBS/Tween
11. Each hydrogel was washed 3 times for 10 minutes each in PBS.	

The stained hydrogels were placed onto a microscope slide and covered with DABCO. An imaging gasket was placed on top of the hydrogel to flatten its top surface. All of the staining was carried out in a darkened room. An aluminum foil cover was placed on top of the 24 well plates to prevent photobleaching of the fluorophores during staining and mounting. Images of the stained slides were taken using a Zeiss LSM 510 Scanning Laser Confocal Microscope. The center, middle and edge regions were imaged from each hydrogel stained. The 'center' region was the area located at the epicenter of

the hydrogel, the point found at the quarter section of the hydrogel. The 'edge' region was located at rounded outer circumference of the hydrogel, opposite to the center region. The 'middle' region was a section of the hydrogel that was equidistant between the center and the edge regions along one of the flattened sides of the hydrogel quarter.

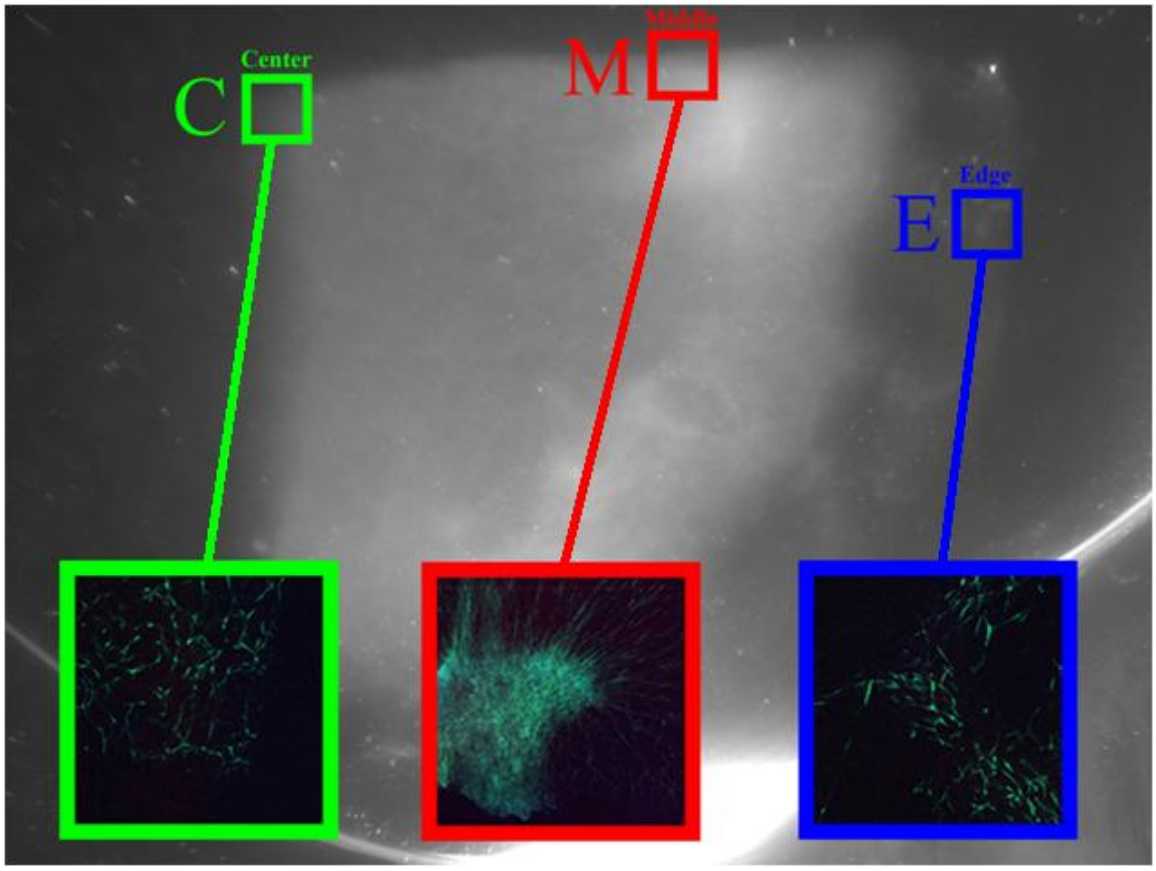

Figure 2.2: An illustration of the three regions analyzed in this project. The 'center' region in green is located where the epicenter of a whole collagen hydrogel. The 'edge' region in blue is the outer most part of a collagen hydrogel , near the circumference. The 'middle' region in red is a region located around the midway point between the center and edge regions.

Chapter 2.4: Thickness Measurements

The 6, 12, 18 and 24 hour inside and on-top rat tail collagen rat NHFC hydrogels were measured for thickness at three points along the radius of each hydrogel quarter. The three points measured were the center, middle and edge regions of a collagen

hydrogel. Flat single edge razor blades were used to cut a slice from the hydrogel quarter. The slice was cut smaller than the thickness of the hydrogel to differentiate the top from the cross section cut. Thickness measurements were made at the center, middle and the edge regions of each hydrogel slice. The total length of the slice was measured in the 6, 12, 18 and 24 hour rat NHFC rat tail collagen hydrogels. Each hydrogel slice was measured using a Zeiss steREO Lumar V. 12 stereomicroscope. Axiovision software was used to capture images of the hydrogel slices and measure the thickness of the slice at each pre-determined point. Using the Measure tool in the Axiovision software, length measurements were taken from images of the hydrogel slice. A line was drawn between the top and bottom surfaces of the hydrogel slice to determine the thickness at a specific point in the hydrogel. The 6, 12, 18 and 24 hour rat NHFC rat tail collagen hydrogels consisted of 1 measurement from 2 quarter segments from 4 different hydrogels at the time points of 6, 12, 18, and 24 hours. Control hydrogels consisted of 500 μl of rat tail collagen hydrogels that were measured for thickness in the center, middle, and edge regions at 6, 12, 18 and 24 hour intervals for comparison with rat NHFC inside and on-top hydrogels. The control hydrogel averages consisted of 1 measurement from each region of 2 quarter segments from 3 different hydrogels at the 6, 12, 18, and 24 hour time ponts. The lengths of both the cell placed (inside and on-top) and control rat NHFC hydrogels were measured for radius length. P values were generated for each set of corresponding hydrogel thicknesses by using a 2 tailed t-test. A two tailed t test was used to compare the control and cellularized hydrogel thicknesses at a specific time point. P values less than 0.05 represented a statistical difference between the control and cellular

hydrogel thickness at that specific region. The error bars surrounding each average was done using the standard deviation of the averages collected from each hydrogel region.

Chapter 2.5 Vimentin Directionality

Confocal images of 3, 6 and 9 hour inside rat NHFC rat tail collagen hydrogels were imported into Image Pro Plus software for angle analysis. Each of the three images were converted into three different RGB color channels. The channel containing the vimentin signal was used to determine cell angle due to the vimentin signal interfering the least with the automated count system of the software. Each cell in the image that had an area of 10 pixels was counted and identified. Some cells were manually separated due to the aggregation of some of the cells in the image. All cells that were identified were also given angle measurements based on their positioning in the image. The angle of each cell was measured by taking the angle formed between the major axis of each cell and comparing it to the vertical. The major axis of each cell is the longest diameter found from the overall shape of the cell. The vertical of an image is a straight line that is found at the middle of the image. A table was created from each image that listed the angle measurement for each identified cell. A histogram based on cell number and each cell's orientation (0 to 180 degrees) was made to determine if a cellular alignment was present in the three regions imaged in inside rat tail collagen hydrogel models.

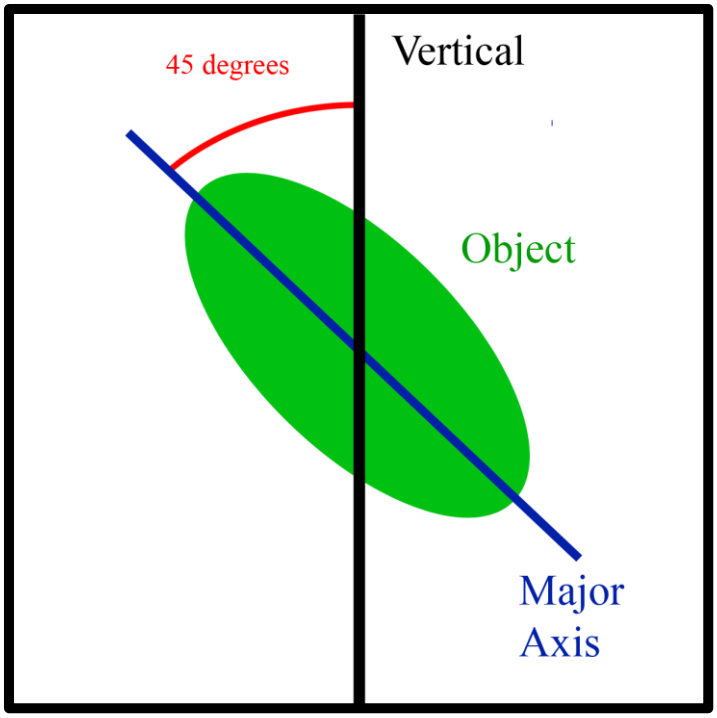

Figure 2.3: Image pro plus compares the vertical and the major axis and calculates an angle measurement based on the angle that lies between the vertical (y-axis) and the major axis of the object.

Chapter 2.6: Observing Cancer Cell-Collagen Hydrogel Interactions

A mouse breast cancer cell line called 4TI-LUC were cultured and placed inside and on-top of bovine type I collagen, rat tail collagen, and human type III collagen hydrogels. The 4TI-LUC cells were cultured in RPMI (Roswell Park Memorial Institute) media supplemented with getamycin, streptomycin, and 10% fetal bovine serum. The 4TI-LUC cell lines had the same cell culture conditions and as the rat NHFCs. All of the 4TI-LUC hydrogels were imaged at 12, 24, and 36 hour time points to observe changes in hydrogel shape.

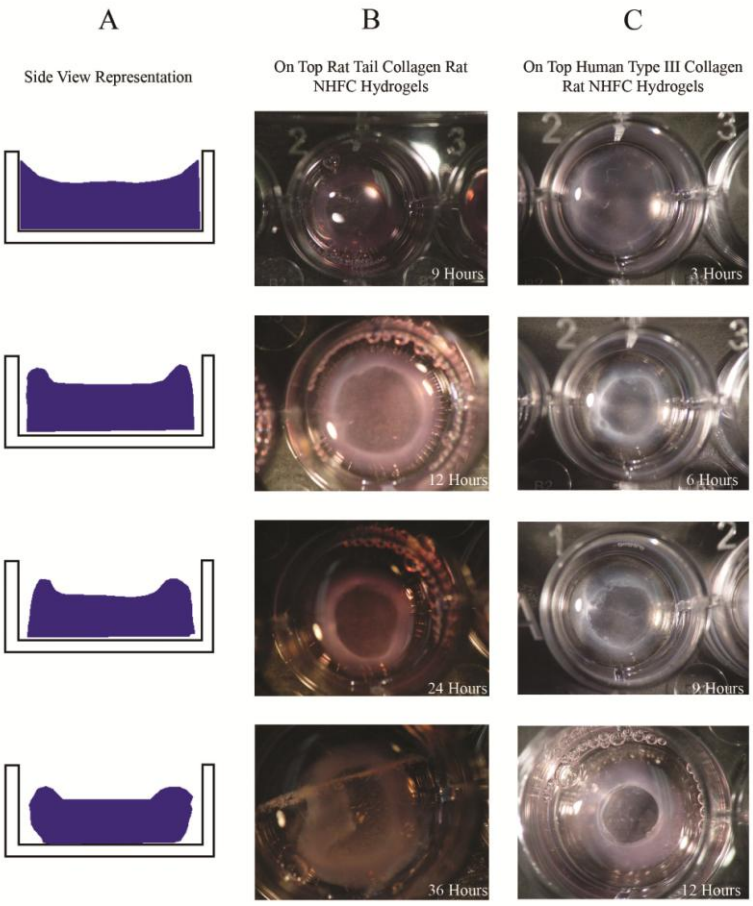

Figure 3.4: On-top placement of rat NHFC remodel collagen hydrogels into a toroid form. Column A contains representations of on-top modeled hydrogels from a side point of view. Columns B and C contain images of hydrogels that have rat NHFC placed on top of them and correspond to the approximations seen in column A. Rat NHFC form toroid shapes when placed on top of human type III collagen and rat tail collagen hydrogels. During toroid formation, the hydrogels shift from a concave shape to a shape resembling an erythrocyte as the cells enter the hydrogel and reorganize. Images correspond to side view representation.

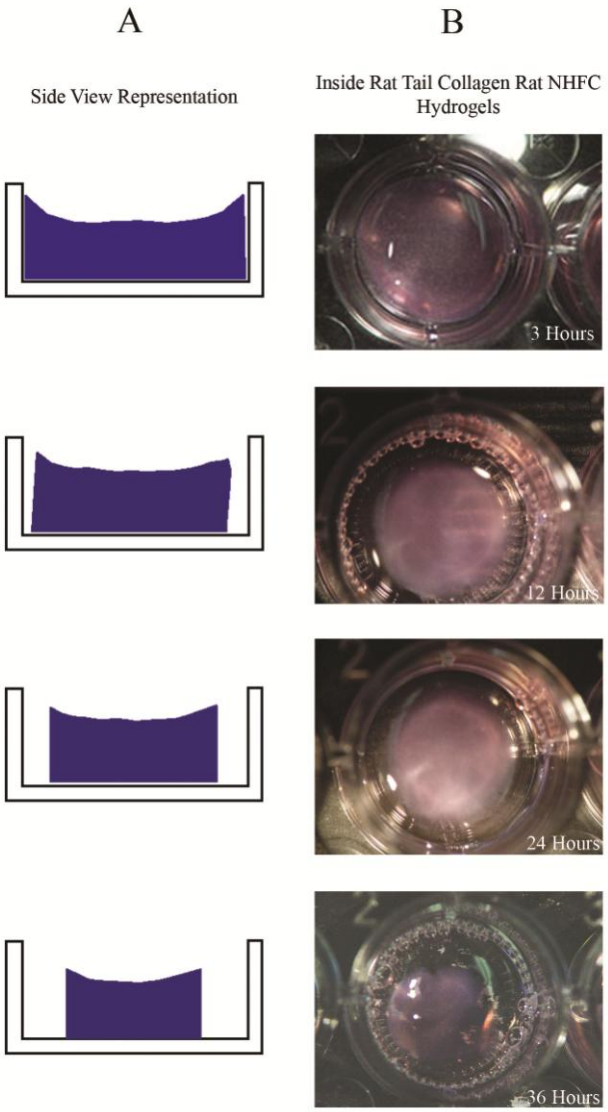

Figure 3.5: Hydrogel contraction caused by placement of rat NHFC inside rat tail collagen hydrogels. Column A contains side view representations of rat NHFC placed inside a rat tail collagen hydrogel. Column B contains overhead images of inside placed rat NHFC rat tail collagen hydrogels. Placement of rat NHFC inside a rat tail collagen hydrogel caused the overall diameter of the hydrogel to shrink over time. The surface of inside-placed rat NHFC rat tail collagen hydrogels became less concave over time. Images correspond to side view representation.

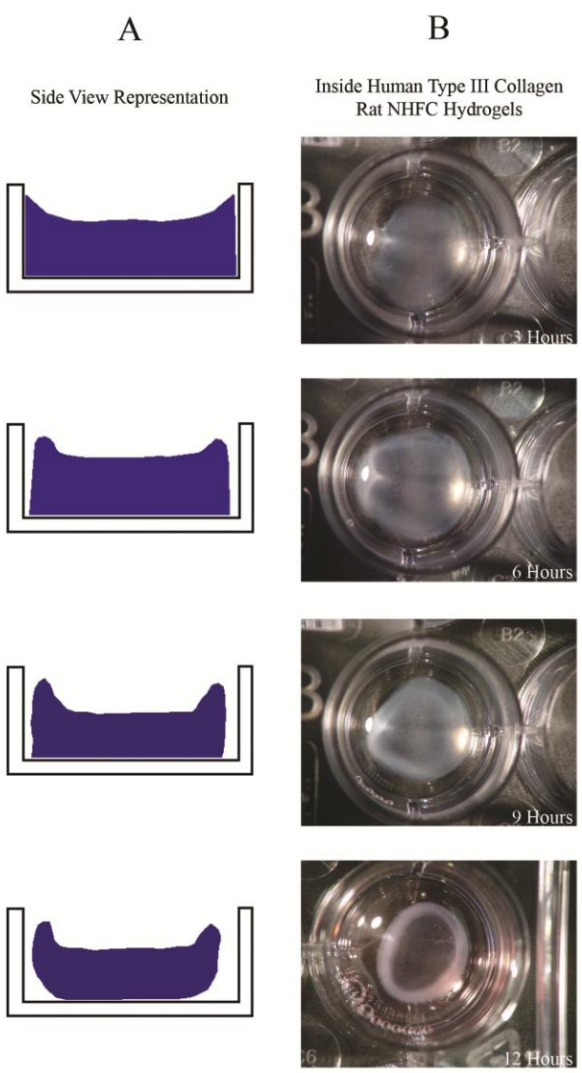

Figure 3.6: Rat NHFC remodel human type III collagen hydrogels into a ring-like shape when placed inside. The 12 hour inside hydrogel in the bottom row have cells accumulated along the edges of the hydrogel, but do not form a toroid shape like cells placed on-top of a collagen hydrogel. Column A contains a side view representation of rat NHFC placed inside of a human type III collagen hydrogel.. Unlike other inside hydrogel models, rat NHFC hydrogels formed a ring like alignment of cells around the edges of an inside type III collagen hydrogel. These hydrogels shrank in diameter similar to other inside-placed hydrogel models. Images correspond to side view representation.

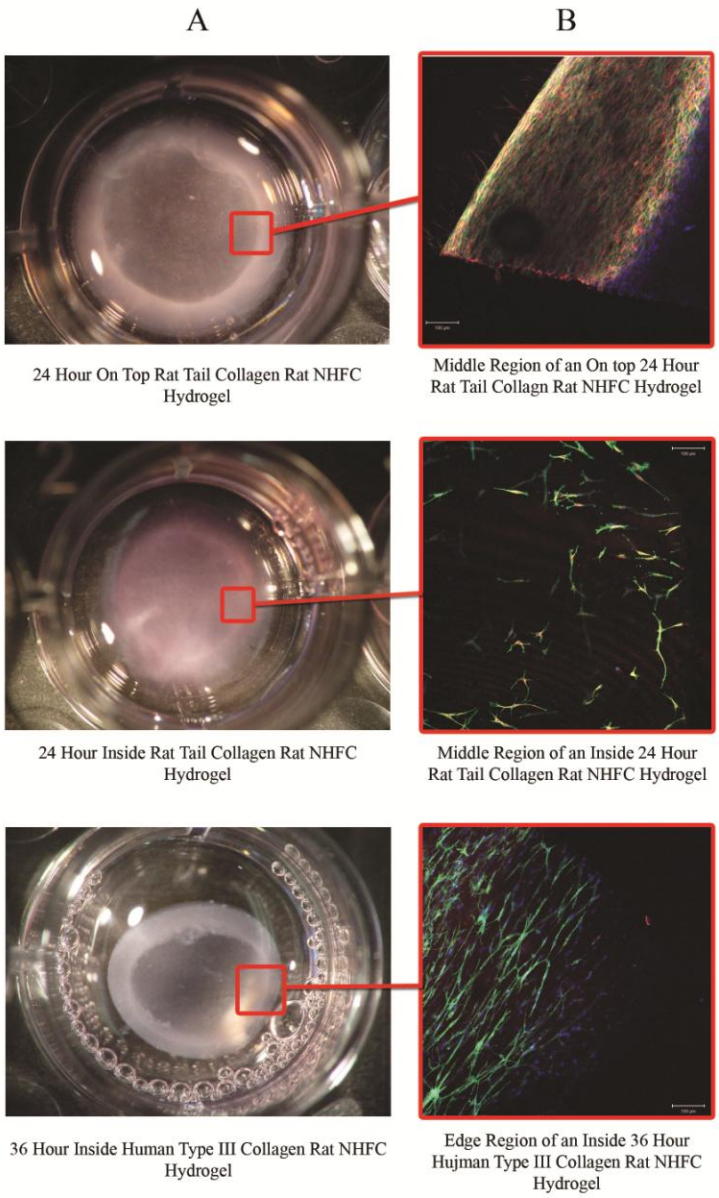

Figure 3.7: Cell alignment could serve as a marker for toroid formation. In all of the confocal images taken, the cell nuclei were stained with DAPI (blue) and f-actin was stained with phalloidin (green). The rat tail collagen hydrogels were stained with a Cy3 conjugated anti vimentin antibody (red). The type III collagen hydrogels were stained with an anti Ki-67 antibody and labeled with at Cy3 conjugated secondary antibody (red).

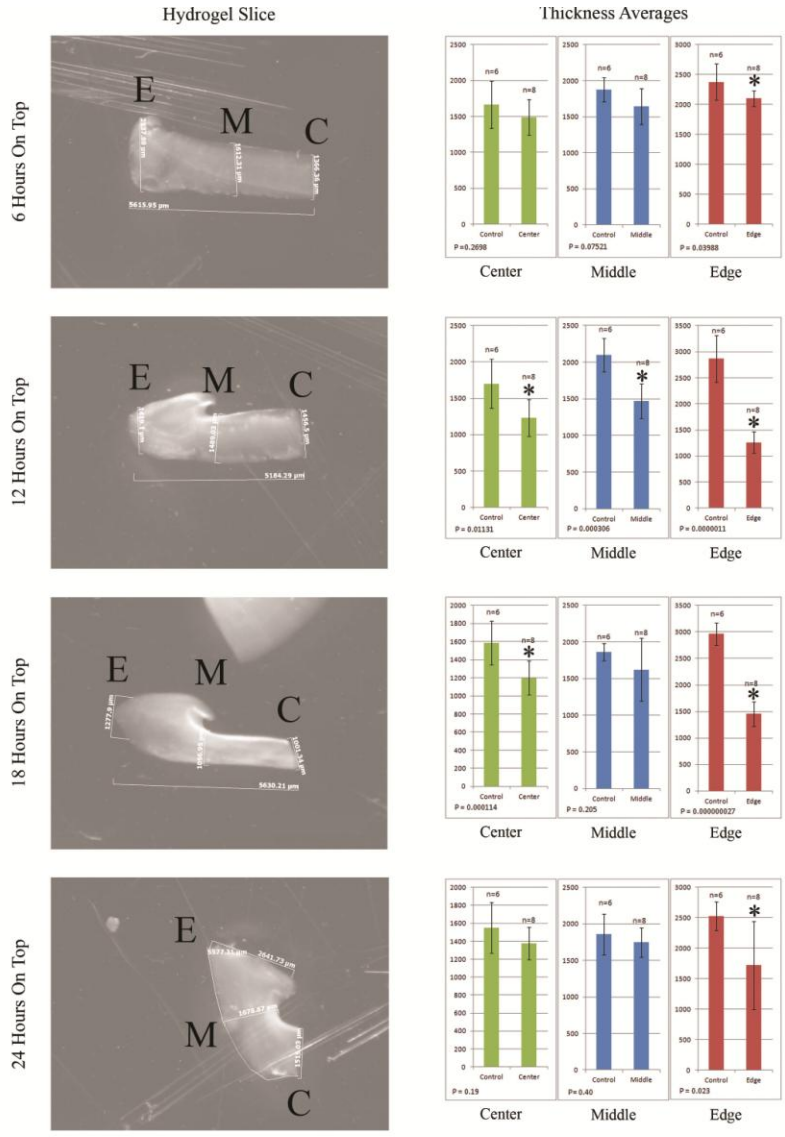

Figure 3.8: The edge and middle regions of on-top hydrogel models became thicker during spheroid formation. The graphs located in the right column correspond to the region at which a hydrogel was measured. Images in the left column are hydrogel slices that were used for thickness measurements. 'C' represents the center region, 'M' represents the middle region and 'E' represents the edge region. The histograms in the right column compare the average thicknesses of the control and cellularized hydrogels. Each bar represents the mean ± SD.

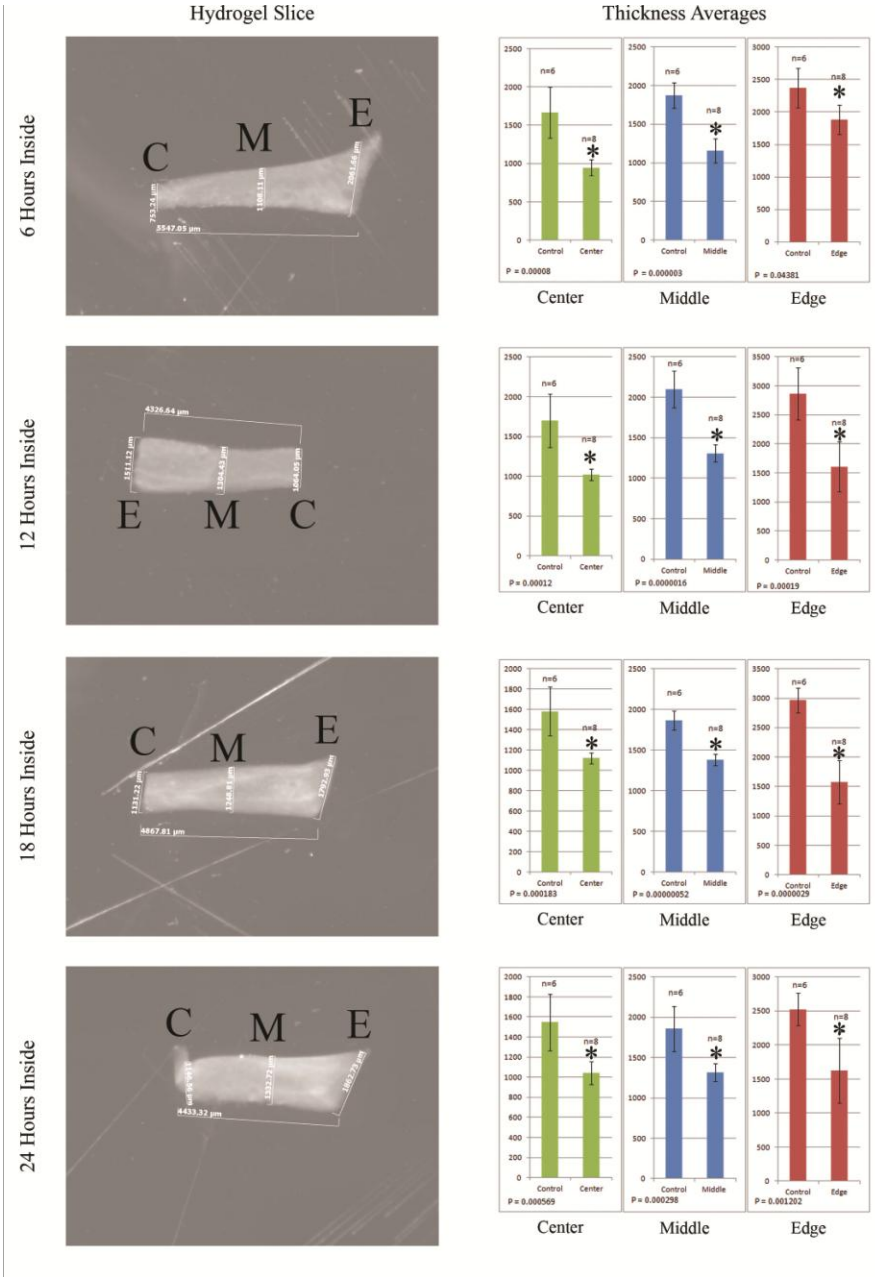

Figure 3.9: The surface of inside rat NHFC hyrogels lose concavity over time. The graphs located in the right column correspond to the region at which a hydrogel was measured. Images in the left column are hydrogel slices that were used for thickness measurements. 'C' represents the center region, 'M' represents the middle region and 'E' represents the edge region. The histograms of each hydrogel type contain control measurements of the same time period that contained no cells. The bars represent mean ± SD.

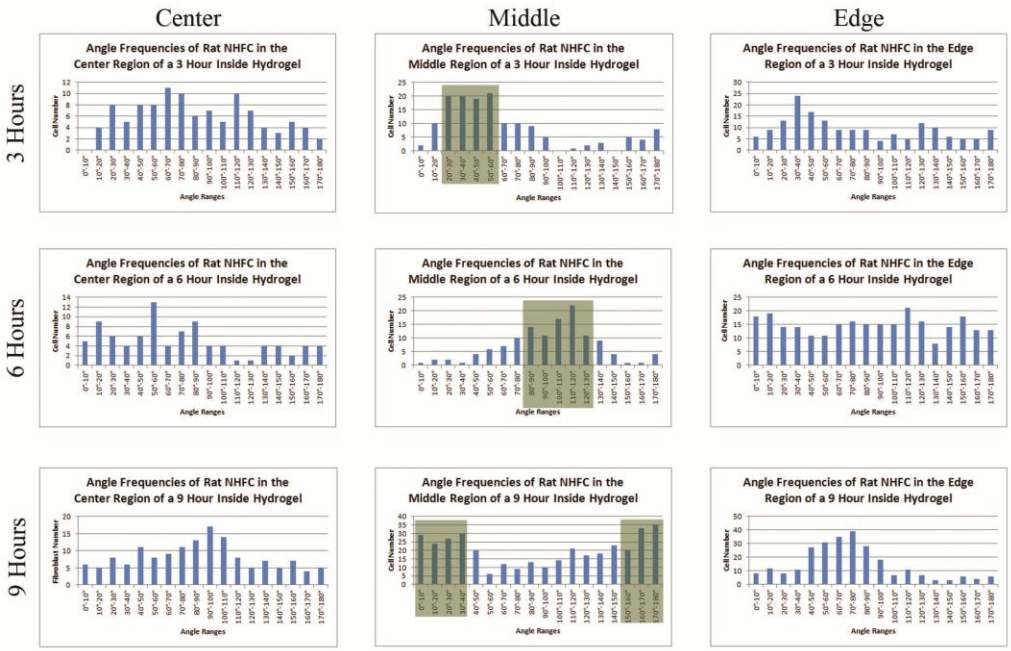

Figure 3.10: The middle region of inside rat NHFC rat tail collagen hydrogels contained patterns of alignment not present in other regions. The middle regions and the edge region of the 9 hour inside hydrogel have a range of angle measurements that contain over half of all of the cells counted in each confocal image.

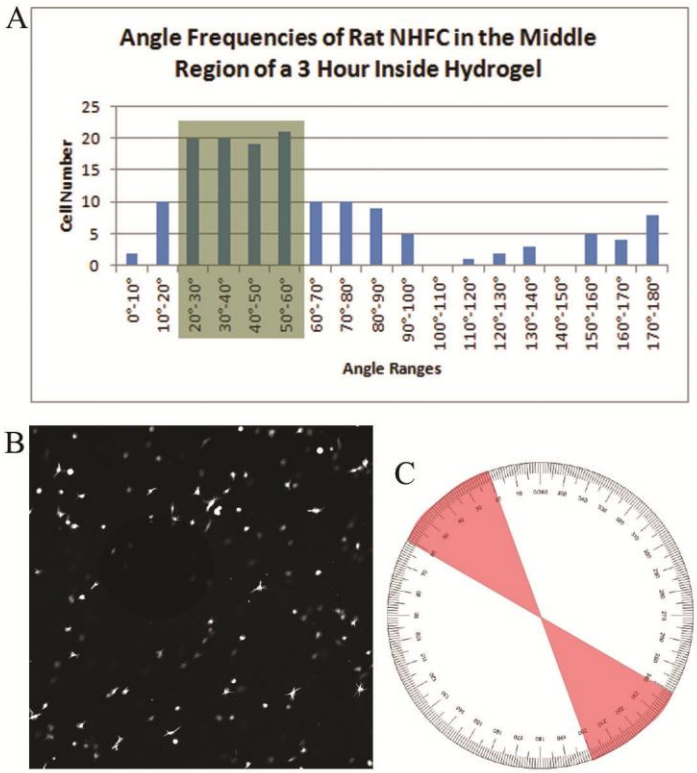

Figure 3.11: The majority of cells in the 3 hour inside rat NHFC middle region confocal image faced the 20° to 60° orientation. The histogram marked 'A' represents the number of cells that were located in each 10° range group. 'B' is an image of the hydrogel region measured where only the vimentin signal is present. 'C' is a graphical representation of where the majority range lies in respect to the confocal image in 'B'.

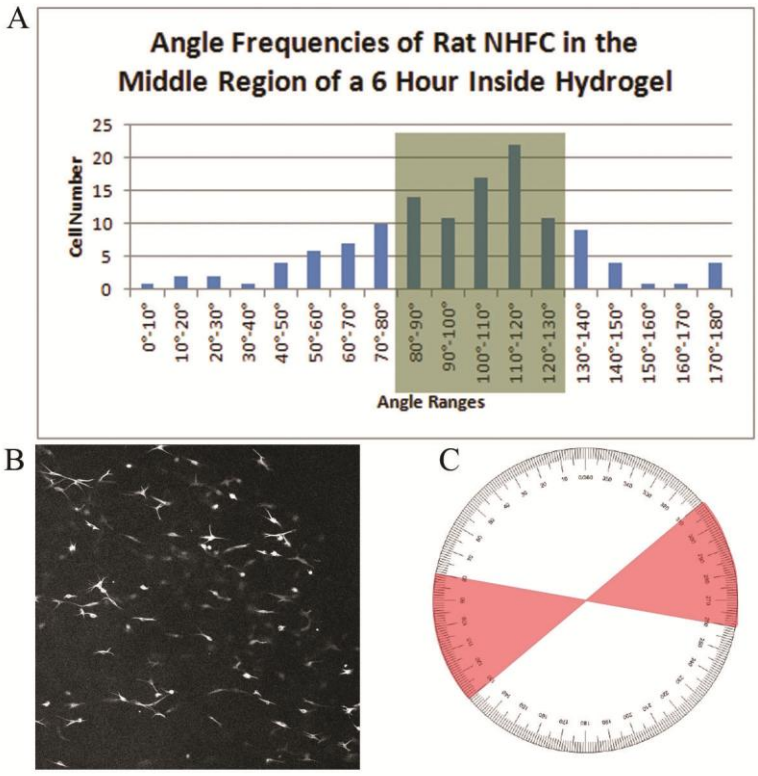

Figure 3.12: The majority of cells were oriented in the 80° to 130° orientation in the middle region of the 6 hour inside rat NHFC rat tail collagen hydrogel. The histogram marked 'A' represents the number of cells that were located in each 10° range group. 'B' is an image of the hydrogel region measured where only the vimentin signal is present. 'C' is a graphical representation of where the majority range lies in respect to the confocal image in 'B'.

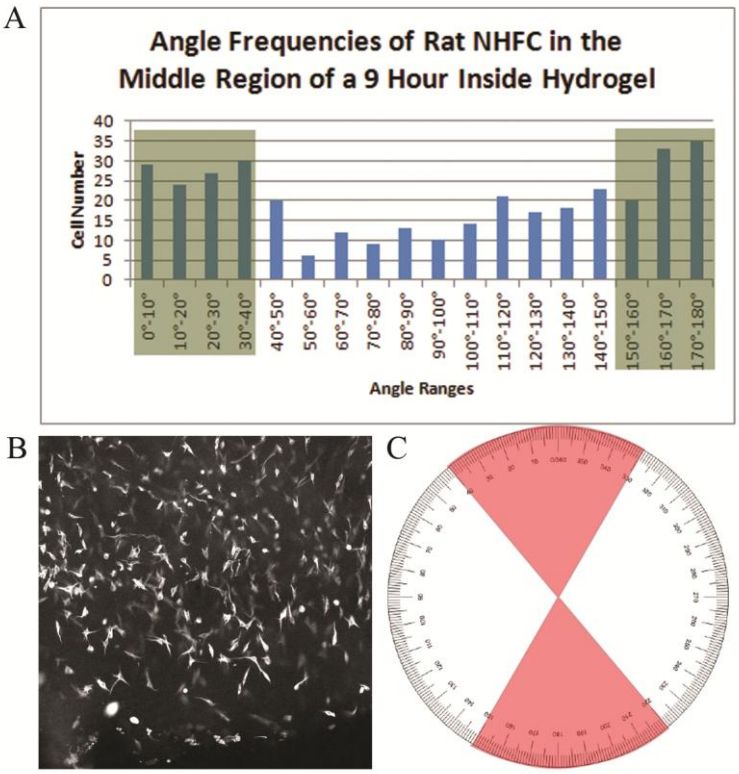

Figure 3.13:The majority of the cells in the middle region of the inside 9 hour rat NHFC rat tail collagen hydrogel were oriented in the 0° to 40° and the 150° to 180° range. The histogram marked 'A' represents the number of cells that were located in each 10° range group. 'B' is an image of the hydrogel region measured where only the vimentin signal is present. 'C' is a graphical representation of where the majority range lies in respect to the confocal image in 'B'.

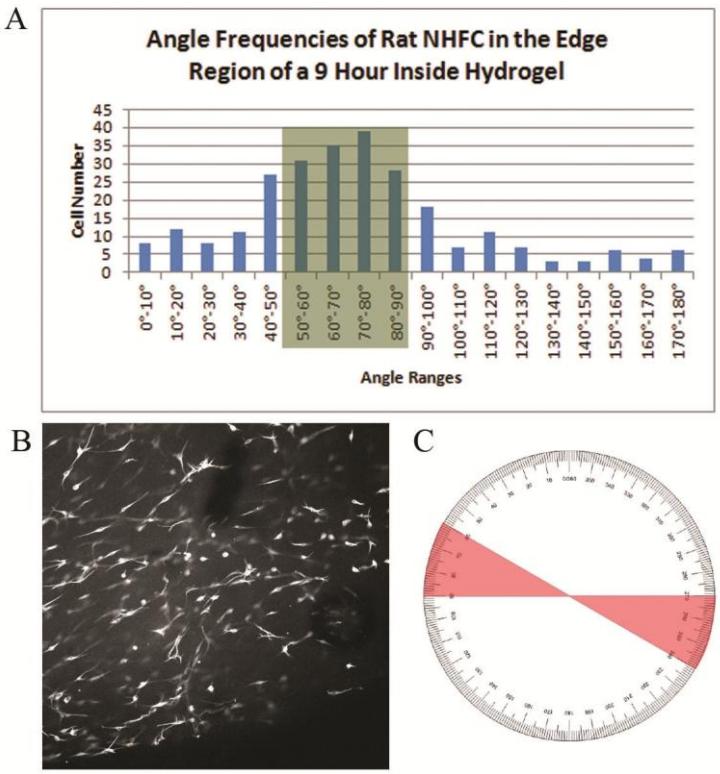

Figure 3.14: The 50° to 90° range contained the majority of cells in the 9 hour rat NHFC rat tail collagen hydrogel edge region. The histogram marked 'A' represents the number of cells that were located in each 10° range group. 'B' is an image of the hydrogel region measured where only the vimentin signal is present. 'C' is a graphical representation of where the majority range lies in respect to the confocal image in 'B'.

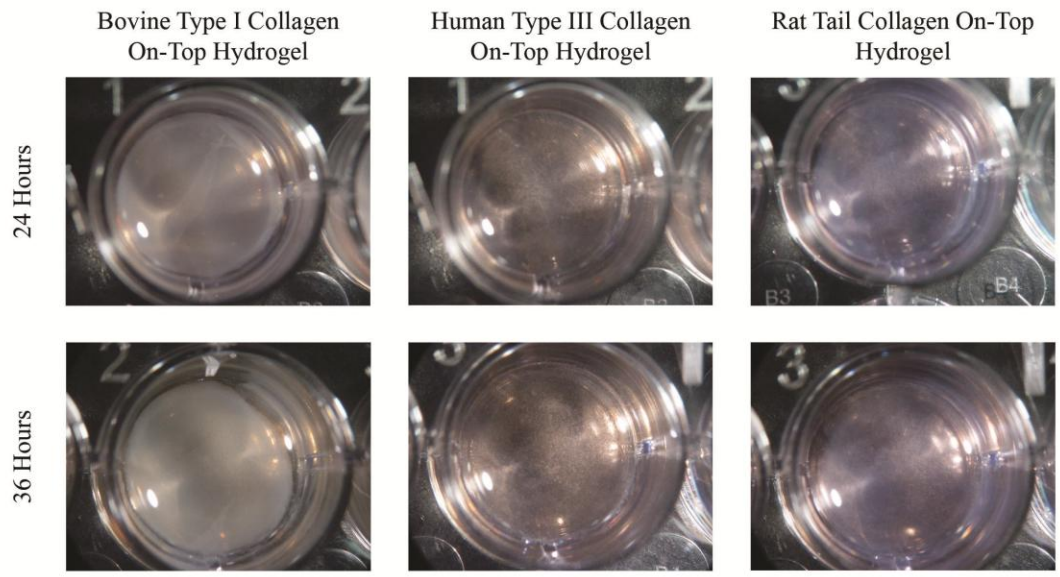

Figure 3.15: Mouse breast cancer cells (4TI-LUC) were placed on-top of Bovine type I, Rat tail, and Human Type III collagen hydrogels. No contraction or toroid formation occurred within 36 hours of hydrogel culture.

Cellularized hydrogels had differing remodeling patterns based upon the placement of the cells and the type of collagen used in the hydrogel (Fig. 3.4 - 3.6). In all uses of rat NHFC and RLEC (Gourdie 2011), when placed on top of a hydrogel, the cells remodeled into a toroid shape. Hydrogels with cells placed on-top are remodeled from a cylindrical form with a concave surface to a shape similar to an erythrocyte (Fig. 3.4). In the on-top placed rat NHFC rat tail collagen hydrogels, the erythrocyte shape was contorted into a spheroid. When rat NHFC and RLEC (Gourdie 2011) were placed inside of rat tail and bovine type I collagen respectively, the hydrogels shrank in diameter, but did not divert from a circular shape (Fig. 3.5). The surface of inside placed hydrogels became less concave the longer the cells were in contact with the hydrogel. Rounded edges and an erythrocyte like shape developed in inside placed rat NHFC human type III collagen hydrogels (Fig. 3.6).

Rat NHFC in on-top hydrogel models formed toroid structures. Normally, when cells are placed inside a hydrogel, the hydrogel shrinks in diameter over time and the cells do not organize into toroid. The cellular alignment present in the on-top human type III collagen hydrogels appeared after 12 hours of incubation (Fig. 3.4). In the case of human type III collagen with rat NHFC mixed in, the hydrogel was gradually remodeled into a ring like shape at the edges of the hydrogel (Fig. 3.6). The cells at the edge regions of the 24 and 36 hour inside type III collagen hydrogels have an alignment similar to toroids, but do not contain the cell density and organization of a toroid made from the on-top placement of cells (Fig. 3.7). Unlike other inside hydrogel models, the cellular alignment in the type III collagen hydrogels was not random at the edge region. The cells in the edge region of the inside placed rat NHFC type III collagen hydrogel were aligned with the edges of the hydrogel that make up the toroid structure. The cellular organization in the edge regions of inside placed Rat NHFC type III collagen hydrogels were not as confluent as the toroids of on-top placed rat NHFC hydrogels.

When rat NHFC were placed on-top of a rat tail collagen hydrogel, the cells remodeled the hydrogel to form a toroid and later a spheroid (Fig. 3.8). When rat NHFC were placed inside a rat tail collagen hydrogel, the hydrogel shrank in diameter and the top surface of the hydrogel became less concave over time (Fig. 3.9). When cells were placed on top of the hydrogel, the edge region became thicker as the hydrogel was remodeled into a spheroid. Between the 12 and 18 hour periods, the middle region was thicker than the edge region due to the inward curving of the edge region of the hydrogel (Fig. 3.8). In some of the spheroid hydrogels measured at the 24 hour time point, the edge region was thicker than the middle region that supported it. Most of the variation seen in

the edge region of the 24 hour on-top hydrogels was due to the hydrogel contorting to form the spheroid. The spheroids that formed in the 24 hour on-top rat NHFC rat tail collagen hydrogels caused the hydrogels to lean to the side. Two sections of the hydrogel from the edge region of the 24 hour on top rat NHFC rat tail collagen hydrogels did not form spheroids and had a middle regions that were thicker than their edges. The other two 24 hour on top sections that did form spheroids had an edge region that was thicker than their middle regions. Statistically the edge regions of on-top cellularized hydrogels were different than the control non-cellularized hydrogels. There was a statistical difference between inside rat tail collagen hydrogels and control rat tail collagen hydrogels at all regions at each time point (Fig. 3.9).

Rat NHFC located in the middle region of the hydrogel had alignment patterns not present in the other two regions. The 3 (Fig. 3.11), 6 (Fig. 3.12), and 9 (Fig. 3.13) hour middle regions and the 9 hour edge region (Fig. 3.14) had varying ranges that contained the majority of the cells in each of the images. The majority range was based on these criteria: the smallest collection of 10° segments that account for over 50% of the total number of cells in the image and the condition that there are no other 10° segments outside the range that are greater than the 10° segments that make up the majority range. The 9 hour inside hydrogel middle region (Fig. 3.13) had more variability than the 3 and 6 hour middle region images. However, the edge region of the 9 hour inside hydrogel (Fig. 3.14) had an alignment with less variability than the middle region. Other than the 9 hour middle region, the other mentioned images fulfilled the requirements needed to determine a majority range.

Chapter 4: Discussion

Chapter 4.1: On-top Hydrogel Placement

The on-top placement of differentiated cell types, such as epithelial and fibroblast cells, cause the remodeling of collagen hydrogels into a toroidal form. Adding specific proteins directly to cells in a collagen environment alters the reorganization of those cells. Previous work from our lab demonstrated that TGFβ-1 (transforming growth factor beta 1) or αCT1 (a C terminal of the gap junction protein connexin 43) supplemented medias can be used to alter the size of the toroid that formed on on-top modeled hydrogels (Gourdie 2011). TGFβ1 upregulates fibrogenic cytokines and molecules that are involved in tissue fibrosis (Saika 2009). αCT-1 is a peptide that increases the size of gap junctions between cells and promotes the healing of cutaneous wounds (Ghatnekar 2009). RLEC on-top hydrogels with TGFβ-1 supplemented media had smaller diameter toroids and contracted more than normal non-media supplemented RLEC on-top hydrogels (Gourdie 2011). Adding αCT1 supplemented media to a RLEC on-top placed type I collagen hydrogel caused the toroid diameter to increase and lower hydrogel contraction (Gourdie 2011). This data indicates that the size of the toroid can be controlled by supplementing the environment with peptides that the diameter of the toroid when placed on top of a collagen hydrogel.

Understanding how cells interact with the surrounding matrix has been a focus of recent research. IPSCs (induced pluripotent stem cell)-derived embryoid bodies are sensitive to changes in substrate stiffness and composition (Macri-Pellazzeri 2015). In breast implants, the coating of the implant can elicit specific reactions from breast fibroblasts (Valencia-Lazcano 2014). The surface in which cells come into contact alters signaling and differentiation processes. The environment that cells are in contact with affect cell differentiation, proliferation and migration patterns. We hypothesized that the collagen surrounding these cells caused different mechanisms of remodeling to occur. Understanding the biochemical changes that occur when cells come into contact with the surface of a collagen hydrogels may lead to a better understanding of the process that causes the cells to reorganize into a toroidal form.

Chapter 4.2: Contraction of Inside Collagen Hydrogels

Interspersing cells throughout a collagen hydrogel caused a different form of remodeling compared to placing cells on-top of a collagen hydrogel. While both on-top and inside placement of Rat NHFC caused overall hydrogel shrinkage, the on-top hydrogel models always reorganized the collagen into a toroid shape, unlike the inside placed rat NHFC hydrogels. From the testing of RLEC, human bone marrow stem cells and rat epicardial cells in inside hydrogel models, it was determined that placing cells inside of a collagen hydrogel resulted in the decrease of the hydrogel diameter over time (Gourdie 2011). Hydrogels of different compositions can shrink or swell based on the external environment. Placing bovine aortic endothelial cells onto a collagen-HEMA (hydroxyethylmethacrylate) hydrogel can cause the cells to produce more type I procollagen than type III collagen (Toselli 1984) Hydrogels containing single stranded

DNA grafted into them shrank when additional single stranded DNA was added (Murakami 2005). The shrinking of the hydrogel was caused by the cross linking between the added single stranded DNA and the DNA on the surface of the hydrogel (Mirakami 2005). Placing sheep fibroblasts and keratinocytes on top of collagen hydrogels caused them to shrink after 8 to 10 days of incubation (Mazzone 2014). Hydrogels made of semi interpenetrating polymer networks of a specific composition shrink considerably at 70°C (Gallagher 2014). Superporous hydrogels made of poly acrylamide-co-acrylic acid shrank or swelled based on the pH levels of the media that they were immersed in (Gemeinhart 2000). Altogether, molecular cross linking, temperature and pH are factors that can cause hydrogels to shrink in size, however, there also seems to be a process where the interaction of cells in conjunction with collagen can cause hydrogel shrinking (Gemeinhart 2000). Here, the diameter reduction observed in the rat tail collagen hydrogels may have been caused by the increase in cell number and the cellular localization within the gel. Control rat tail collagen hydrogels without any differentiated cells showed no major changes after 24 hours of incubation in media. Rat tail collagen hydrogels that contained rat NHFC placed inside of them shrank in diameter as the cells proliferated and changed into a spindle like shape over time (Fig. 3.7). The cells that are placed inside and on top of the hydrogel cause collagen hydrogel remodeling. Rat NHFCs and other differentiated cell types may induce a chemical or physical change to the collagen environment surrounding it, that enhances cell reorganization and migration. The inside placed rat NHFC hydrogels do not change form other than shrinking in size, so the cells may migrate from the edges toward the center of the hydrogel. In both inside and on-top hydrogel models, the cells and their placement control hydrogel remodeling.

Chapter 4.3: Type III Collagen and Cellular Reorganization

Type I collagen is the most abundant type of collagen found in the human body. Type I collagen can be found in bones, tendon ligaments and blood vessels. Type III collagen is the second most abundant collagen type in the human body. Type III collagen is normally co-localized with type I collagen and is present in blood vessels, elastic tissues, skin, and the walls of hollow organs. Rat NHFC placement inside and on-top of human type III collagen is similar to the on-top placement of other differentiated cell types on type I collagen hydrogels. Cellular toroids were created in all on-top modeled collagen hydrogels. Unlike the inside placed rat NHFC rat tail collagen hydrogels, when rat NHFCs were placed inside human type III collagen hydrogels, a circular alignment of cells formed around the edges of the hydrogel, similar to when differentiated cells were placed on-top of a collagen hydrogel.

The mechanism of collagen utilization by differentiated cells may vary based on the type of collagen that it comes in contact with. Type III collagen overexpression in rat hearts led to an increase in extracellular matrix expansion (Schuman 2014). The amount of type III collagen around the heart could play a factor in how neonatal heart fibroblasts utilize collagen. 20% of myocardial collagen is composed of the type III form (Laviades 1994). Type III collagen is present in higher amounts in rat fetal skin than in normal adult rat skin (Merkel 1988). Type III collagen found in granulation tissues were double in size in fetal skin injuries and only had a small increase in adult skin granulation tissues (Merkel 1988). Fetal cell types may be able to reorganize better in type III collagen than in type I collagen. It may be possible for some cell types to migrate and organize differently based on collagen environment. The inside placement of rat NHFC in type III collagen resulted in the hydrogel remodeling into a ring like form. The ring shape formed

from the inside hydrogel was located at the edge region of the hydrogel (Fig. 3.6) as compared to the toroids that appeared in the middle region in on-top models (Fig. 3.4). The alignments of the cells at the edge region of the inside rat NHFC rat tail collagen hydrogel are similar to the alignment present in the toroid found in the middle regions of on top rat NHFC collagen hydrogels (Fig. 3.7). The ring like alignment of cells remodel the hydrogel into an erythrocyte like shape (Fig. 3.6) The placement and cell type are important factors in determining the modulation of type III collagen hydrogels.

Chapter 4.4: Collagen Types and Cellular Reorganization

The collagen that surrounds the rat NHFCs can greatly influence reorganization and collagen modulation. Rat NHFCs were able to reorganize differently when surrounded by human type III collagen than rat tail collagen. Rat NHFC placed inside of human type III collagen hydrogels gradually reorganized from a random to an organized orientation. Rat NHFC may have receptors that have a higher affinity for type III collagen than other types of collagen. Two days after wounding rat skin tissue, both fetal and adult granulation tissues contained higher amounts of type III collagen than normal uninjured tissue (Merkel 1988). Rat NHFC reorganization may not be fully optimized in human type III collagen. After 36 hours of incubation, spheroids did not form in on-top models of rat NHFC human type III collagen hydrogels, while in rat tail collagen on-top rat NHFC models, spheroid formation occurred between the 18 and 24 hour time points. Rat tail collagen may be a factor in causing the rat NHFC to remodel the hydrogel into a spheroid form within 24 hours. Rat NHFCs may be able to manipulate collagen and reorganize based on the type and total amount of surrounding collagen. Type III collagen supported rat NHFC inside hydrogel reorganization, while the rat tail collagen supported

spheroid formation in on-top hydrogel models. In designing cell constructs with collagen scaffolds, the collagen and cell type will affect how the collagen is remodeled and the form that the cells reorganize into.

Chapter 4.5: Cellular Collagen Receptors

Integrins are transmembrane cell adhesion proteins that bind the ECM to the cytoskeleton. Integrins mediate the interactions between the cytoskeleton and the ECM and allow cells to bind to and modulate the matrix. Through integrins, ECM proteins like collagen and fibronectin can be bound and utilized by cells. Integrins are made up of a combination of α and β subunits. $\alpha_1\beta_1$ integrins bind monomeric type I collagen to the cell cytoskeletion (Jokinen 2004). $\alpha_2\beta_1$ integrins are functional cellular receptors that mediate the spreading of the cellular cytoskeleton on fibrillar type I collagen (Jokinen 2004). $\alpha_2\beta_1$ integrins promote the formation of long cellular projections onto fibrillar type I collagen and support contraction of fibrillar collagen hydrogels (Jokinen 2004). Type III collagen contains a binding site for the $\alpha_1\beta_1$ and $\alpha_2\beta_1$ integrins (Kim 2005). The GROGER sequence motif in type III collagen can bind with the l domains of the α_1 and α_2 subunits of integrins. Synthetic peptides that have the GROGER sequence can serve as a substrate for integrin dependent cell adhesion (Kim 2005). Discoidin domain receptors (DDR) are receptor tyrosine kinases that recognize collagen as ligands and regulate cell to collagen interactions (Fu 2013). The DDR2 Fc region can bind to four different peptide regions in human type III collagen (Xu H 2011). It is possible for cells to bind to type III collagen through integrins and DDR2 can recognize and bind to human type III collagen. Finding the receptors rat NHFC use to interact and remodel type III collagen could determine

what causes the spheroid remodeling observed in rat NHFC Human type III collagen hydrogel models.

Chapter 4.6: Contraction and Cell Alignment

The thickness and overall shape of each hydrogel changed based on cell placement and collagen type. Hydrogel contraction was present in both on-top and inside hydrogel models. Contraction may be a major factor that contributes to the physical changes the hydrogels. The shrinking of inside placed hydrogels and the spheroid formation of on-top hydrogels may be linked by cell mediated contraction. The changes in cell shape and size in inside rat NHFC hydrogels developed simultaneously with the shrinking diameter of inside rat NHFC hydrogels. The levels of contraction may be dependent on cell proliferation and confluency. Cells in on-top placed hydrogels proliferated quickly and became confluent (Fig. 3.7). Rat NHFC progressively shifted into a elongated spindle shape in inside hydrogel models, and as the hydrogel shrank, the cells became more clustered and organized (Fig. 3.7). The rate at which cells can aggregate in collagen may be a controlling factor in how the hydrogels are remodeled. Hence, cell aggregation may be the controlling factor in collagen hydrogel remodeling.

Chapter 4.7: Cell Alignment, Toroid Thickness and Spheroid Formation

The thickness of the hydrogel in each of the on-top rat tail collagen rat NHFC hydrogels shifted over time depending on toroid or spheroid formation. The shifts in collagen thickness may be related to the migration and orientation of cells in respect to the hydrogel. At the 6 hour time point, there was little to no modulation of the collagen hydrogel in both on-top (Fig. 3.8) and inside (Fig. 3.9) hydrogel models. After 6 hours, the thickness of the hydrogel at the three measured regions shifted based on the initial

placement of the cells. Inside placed rat NHFC hydrogels shrank gradually in surface area and a loss of concavity on the surface of the hydrogel was apparent. The loss of concavity from the center to the edge regions of inside placed rat NHFC rat tail hydrogels could have been caused by the clustering of cells at later stages of cell culture. The shifting of collagen thickness in on-top hydrogels may be due to the formation of toroids. During toroid formation, the middle region gradually thickens and the edge region is remodeled into a curved form that is not as thick as the initial edge region (Fig. 3.8). If the hydrogel does not form into a spheroid, the middle region, where the toroid forms contains the highest thickness of collagen. When a spheroid develops from a toroidal form, on average, the edge region becomes thicker than the middle region. These shifts in thickness between toroid and spheroid formation in on-top hydrogels may indicate how collagen is reorganized by rat NHFCs and other differentiated cell types. The middle and edge regions fluctuate the most in on-top hydrogel models. In inside hydrogel models, there was a statistical difference between the cellularized and the non-cellularized control at all regions and time points (Fig. 3.9). The inside hydrogels gradually became thicker at the center regions and thinner at the edge regions, causing a decrease in conavity of the surface of inside hydrogels over time.

Cell alignment patterns could serve as a marker for spheroid and toroid formation in hydrogels. The middle region was where cell alignment was first observed in inside hydrogels and is the region where the toroid forms in on-top hydrogel models. The contraction of the on-top hydrogel models may be linked to the alignment of cells in the toroid. The rat NHFCs that were placed on top and integrated into the surface of the on-top hydrogels may fuel the transition of the hydrogel into a spheroid shape. The middle

region may also have a role in spheroid formation, as collagen relocates toward the middle region before spheroid formation (Fig. 3.8). The center region does not seem to contribute much to toroid or spheroid formation, however, in all of the hydrogels that were remodeled into spheroids, cells were heavily clustered in the center region of spheroid shaped hydrogels. Cellular coverage of the hydrogel and toroid formation seem to be vital stages that are needed for spheroid formation.

Chapter 4.8: Future Directions

These results show that collagen type and cell placement are important factors that determine how collagen is remodeled to accommodate cellular reorganization. There are physical differences between the inside and on-top hydrogel models that can limit or enhance cellular reorganization and collagen remodeling. Determining the mechanism of self assembly in collagen could lead to controlling cellular aggregation in other inside placed hydrogel models with different cell types. Understanding the biochemical changes that occur between the inside placement of rat NHFC in rat tail collagen and human type III collagen is critical to deciphering how these cell types self aggregate. Rat NHFCs may have specific receptors that allow for better migration in type III collagen. Finding a factor that promotes spheroid formation could be used to control the reorganization of cells in other hydrogel formats such as pAA (poly acrylic acid). One observation that was made was that the cancerous 4TI-LUC cells did not self assemble or reorganize collagen in any of the collagen hydrogels made in this project (Fig. 3.15). Understanding how cancer disrupts cell migration and aggregation patterns could lead to a better understanding of how non-cancerous cells organize and migrate on the surface and inside of collagen hydrogels.

Chapter 5: Conclusion

We hypothesized that the cell type and the collagen environment have an impact on how cellularized collagen hydrogels were remodeled. Rat NHFCs were observed in rat tail collagen and human type III collagen hydrogel types. The changes in hydrogel thickness between inside and on-top placed rat NHFC hydrogels was examined at three different regions along the hydrogel radius. Cell alignment was measured from vimentin orientation in rat NHFC inside hydrogel models. Regardless of the collagen type, when non-cancerous cells were placed on top of a collagen hydrogel, a toroid formed. Cell type and collagen type may determine how cells reorganize inside of collagen hydrogels. Rat NHFCs placed inside human type III collagen hydrogels can reorganize along the edges of the hydrogel and cause the hydrogel to form into a spheroid shape, a pattern not seen in any other inside celluarized hydrogel model. The majority of cells in the middle and edge regions of inside rat NHFC rat tail collagen hydrogels displayed an alignment. Cellular alignment patterns may shift from the middle region to the edge region over time in inside modeled rat NHFC rat tail collagen hydrogels. There may be chemical or genetic expression changes that could affect how cells reorganize in collagen. Understanding the differences between how rat NHFC remodel type I and type III collagen could lead to understanding why this cell type is able to reorganize inside collagen hydrogels effectively. Cells placed inside a collagen hydrogel reorganize differently based on their positioning and environment. We also observed that cancer

cells do not reorganize or remodel collagen hydrogel regardless of collagen type or cellular positioning. Understanding the factors that cause toroid and spheroid formation could allow cells to reorganize in sub-optimal environments. Knowing the factors that can enhance toroid and spheroid formation of differentiated cells can lead to improvements in future tissue engineering projects.

References

Antoine, E., Vlachos P., & Rylander, M. (2014). Review of Collagen I Hydrogels for Bioengineered Tissue Microenvironments: Characterization of Mechanics, Structure, and Transport. *Tissue Engineering Part B: Reviews. 20(6), 182-196.* doi: 10.1089/ten.TEB.2014.0086.

Artym, V.V., & Matsumoto, K. (2010). Imaging cells in three-dimensional collagen matrix. *Current Protocols in Cell Biology.Chapter 10: Unit 10.18: 1-20.* doi: 10.1002/0471143030.cb1018s48.

Blanplain, C., & Fuchs, E (2006). Epidermal stem cells of the skin. *Annual Review of Cell and Developmental Biology. 22:339-373* PMID:1682

Cen, L., Liu, W., Cui, L., Zhang, W., & Cao, Y (2008). Collagen Tissue Engineering: Development of Novel Biomaterials and Applications. *Pediatric Research. 63(5), 492-496*. doi: 10.1203/PDR.0b013e31816c5bc3

De Castro Bras, L.E., Proffitt, J.L., Bloor, S., & Sibbons, P.D. (2010). Effect of crosslinking on the performance of a collagen-derived biomaterial as an implant for soft tissue repair: a rodent model. *Journal of Biomedical Materials Research Part B. 95(2): 239-49*. doi: 10.1002/jbm.b.31704.

Dewavrin, J.Y., Hamzavi, N., Shim. V. P. W., & Raghunath, M. (2014). Tuning the architecture of three dimensional collagen hydrogels by physiological

macromolecular crowding. *Acta Biomaterialia. 10(10). 4351-9.* doi: 10.1016/j.actbio.2014.06.006

Di Lullo, G., Sweeney, S., Korkko, J., Ala-Kokko, L., & San Antonio J.D. (2002). Mapping the Ligand-binding Sites and Disease-associated Mutations on the Most Abundant Protein in the Human, Type I Collagen. *Journal of Biological Chemistry. 277(6). 4223-4231.* doi:10.1074/jbc.M110709200

Dong, N., Xu, B., Benya, S., & Tang, X. (2014). MiRNA-26b inhibits the proliferation, migration, and epithelial-mesenchymal transition of lens epithelial cells. *Molecular and Cellular Biochemistry. 396(1-2). 229-38.* doi: 10.1007/s11010-014-2158-4.

Dunphy, S. E., Bratt, J., Akram, K. Forsyth, N., & El Haj, A. (2014). Hydrogels for lung tissue engineering: Biomechanical properties of thin collagen–elastin constructs. *Journal of the Mechanical Behavior of Biomedical Materials. 38. 251-9.* doi: 10.1016/j.jmbbm.2014.04.00

Eckes, B., Colucci-Guyon, E., Smola, H., Nodder, S., Babinet, C., Krieg, T., & Martin, P. (2000). Impared wound healing in embryonic and adult mice lacking vimentin. *Journal of Cell Science. 113 (pt13). 2455-62.*

Frantz C, Stewart Km, Weaver Vm. The extracellular matrix at a glance. Journal of Cell Science. 2010 Dec 15; 123(pt 24): 4195-4200.

Fu, H.L., Valiathan, R.R., & Arkwright, R.(2013). Discoidin domain receptors: unique receptor tyrosine kinases in collagen-mediated signaling. *Journal of Biological Chemistry. 288(11). 7430-7.* PMID: 23335507.

Gallagher, S., Florea, L., Fraser, K. J., & Diamond, D. (2014). Swelling and shrinking properties of thermo-responsive polymeric ionic liquid hydrogels with embedded linear pNIPAAM. *International Journal of the Molecular Sciences. 159(4). 5337-49.* doi:

Gemeinhart, R.A., Chen, J., Park, H.,& Park, K.. pH-sensitivity of fast responsive superporous hydrogels. *Journal of Biomaterials Science Polymer Edition. 11(12). 1371-80.* doi:10.3390/ijms15045337

Ghatnekar, G.S., O'Quinn, M.P., Jourdan LJ, Gurjarpadhye AA, Draugnhn RL, Gourdie, R.G. (2009). Connexin 43 carboxyterminal peptides reduce scar progenator and promote regenerative healing following skin wounding. *Regenerative Medicine. 4(2). 205-23.* doi: 10.2217/17460751.4.2.205.

Gourdie, R.G., Myers, T.A., McFadden, A., Li, Y.X., & Potts, J.D. (2012). Self-Organizing tissue engineered constructs in collagen hydrogels. *Microscopy and Microanalysis. 18(1). 99-106*. doi: 10.1017s/S1431927611012372.

Jakab, K., Neagu, A., Mironov, V., Markwald, R., Forgacs, G. (2004). Engineering biological structures of prescribed shape using self-assembling multicellular systems. *PNAS 101(9). 2864-2869.* doi: 10.1073/pnas.0400164101

Jeyanthi, R., Rao, K.P. (1990). In vivo biocompatibility of collagen-poly(hydroxyethyl methacryate) hydrogels. *Biomaterials 11(4). 238-43*. PMID: 2200533

Jokinen, J., Dadu. E., Nykvist, P., Kapyla, J., White, D.J., Ivaska, J. Vehvilainen, P., Reunanen, H., Larjava, H., Hakkinen, L., & Heino, H. (2004). Integrin-

mediated cell adhesion to type I collagen fibrils. *Journal of Biological Chemistry. 279(30). 31956-63*. doi: 10.1074/jbc.M401409200

Kalluri, R., & Weinburg, R. (2009). The basics of epithelial-mesenchymal transition. *The Journal of Clinical Investigation. 119(6). 1420-1428.* doi:10.1172/JCI39104

Kim, J.K., Xu, Y., Xu, X., Keene, D.R., Gurusiddappa, S., Liang, X., Wary, K.K., & Hook, M. (2005). A novel binding site in collagen type III for integrins alpha1beta1 and alpha2beta2. Journal of Biological Chemistry. 280(37). 32512-20. doi:10.1074/jbc.M502431200.

Laviades, C., Mayor, G., & Diez, J. (1994). Treatment with lisinopril normalizes serum concentrations of procollagen type III amino-terminal peptide in patients with essential hypertension. American Journal of Hypertension. 7(1). 52-8. doi: 10.1093/ajh/7.1.52

Liu, X., Wu, H., Byrne, M., Krane, S., & Jaenisch, R. (1997). Type III collagen is crucial for collagen I fibrillogenesis and form normal cardiovascular development. *PNAS. 94(5) 1852-1856.*

Macri-Pellizzeri, L., Pelacho, B., Sancho, A., Iglesias-Garcia, O., Simon-Yarza, A.M., Soriano-Navvaro, M., Gonzalez-Granero, S. Garcia-Verdugo, J.M., De-Juan-Pardo, E.M., & Prosper, F. (2015). Substrate stiffness and composition specifically direct differentiation of induced pluripotent stem cells. Tissue Engineering Part A. 21(9-10) 1633-41. doi: 10.1089/ten.TEA.2014.0251.

Mazzone, L., Pontigga, L., Reichmann, E., Ochsenbein-Kolble, N., Moehrien, U., & Meuli, M. (2014). Experimental tissue engineering of fetal skin. *Pediatric Surgery International. 30(12). 1241-7*. doi: 10.1007/s00383-014-3614-7

Merkel, J.R., DiPaolo, B.R., Hallock, G.G., & Rice, D.C. (1988). Type I and type III collagen content of healing wounds in fetal and adult rats. *Proc Soc Exp Biol Med. 187(4):493-7*. PMID: 3353398

Mizuno, K., Boudko, S., Engle, J., & Bachinger, H.P. (2013). Vascular Ehlers-Danlos syndrome mutations in type III collagen differently stall triple helical folding. *Journal of Biological Chemistry. 288(26). 19166-76.* doi: 10.1074/jbcM113.462002

Murakami, Y., & Maeda, M. (2005). DNA-responsive hydrogels that can shrink or swell. *Biomacromolecules. 6(6). 2927-9*. doi:10.1021/bm0504330

Park, J.W., Kang, Y.D., Kim, J.S., Lee, J.H., & Kim, H.W. (2014). 3D microenvironment of collagen hydrogel enhances the release of neurotrophic factors from human umbilical cord blood cells and stimulates the neurite outgrowth of human neural precursor cells. *Biochemical and Biophysical Research Communications. 477(3). 400-406.* doi: 10.1016/j.bbrc.2014.03.145

Saika, S., Yamanaka, O., Okada, Y., Tanaka, S., Miyamoto, T., Sumioka, T., Kitano, A., Shirai, K. & Ikeda, K. (2009). TGF beta in fibroproliferative diseases in the eye. Frontiers in bioscience. 1. 376-90. https://www.bioscience.org/2009/v1s/af/32/fulltext.htm

Satelli, A., & Li, S. (2011). Vimentin in cancer and its potential as a molecular target for cancer therapy. *Cellular and Molecular Life Sciences. 68(18). 3033-46.* doi: 10.1007/s00018-011-0735-

Scholzen, T., & Gerdes, J. (2000). The KI-67 protein: from the known to the unknown. *Journal of Cell Physiology. 182(3) 311-22.* doi: 10.1002/(SICI)1097-4652(200003)182:3<311::AID-JCP1>3.0.CO;2-9

Schumann, M.L., Perez Diaz, L.S., Landa, M.S., Toblli, J.E., Cao, G, Alvarex, A.L., Finielman, S., Pirola, C.J, & Garcia, S.I. (2014). Thyrotropin-releasing hormone overexpression induces structural changes of the left ventrical in the normal rat heart. *American Journal of Physiology: Heart and Circulatory Physiology. 307(11). H1667-74*. doi: 10.1152/ajpheart.00494.2014

Toselli, P., Mogayzel, P., Faris, B., Ferrera, R., Franzblau, C. (1984). Mammalian cell growth on collagen hydrogels. *Scanning Electron Microscopy. 1984. Part. III. 1301-12.*

Valencia-Lazcano, A.A., Alonso-Rasgado, T., & Bayat, A. (2014). Physio-chemical characteristics of coated silicone textured versus smooth breast implants differentially influence breast-derived fibroblast morphology and behavior. *Journal of the mechanical behavior of biomedical materials. 40. 140-55*. doi: 10.1016/j.jmbbm.2014.08.018

Whitesides, G.M., & Grzybowski, B. (2002). Self-Assembly at All Scales. *Science. 295(5564). 2418-2421*. doi: 10.1126/science.1070821

Xu, H., Raynal, N., Stathopoulous, S., Myllyharju, J., Farndale, R.W., & Leitinger, B. (2010). Collagen binding specificity of the discoidin domain receptors:

binding sites on collagens II and III and molecular determinants for collagen IV recognition by DDR1. *Matrix Biology. 30(1). 16-26.* doi: 10.1016/j.matbio.2010.10.004.

Yan, C., Grimm, W., Garner, W., Qin, L., Travis, T., Tan, N., & Han, Y. (2010). Epithelial to Mesenchymal Transition in Human Skin Wound Healing is Induced by Tumor Necrosis Factor-α through Bone Morphogenic Protein-2. *American Journal of Pathology. 176(5). 2247-2258*. doi: 10.2353/ajpath.2010.090048